Citation: GAO Zhiwei, ZHANG Cong, LI Meijun, FANG Ronghui, BORJIGIN Tenger, XIAO Hong, ZHU Zhili. Application of laser Raman spectroscopic parameters of coal maceral analysis with different maturity [J]. Petroleum Geology & Experiment, 2022 (4): 705–719.

Application of laser Raman spectroscopic parameters of coal maceral analysis with different maturity

GAO Zhiwei[1,2], ZHANG Cong[3,4], LI Meijun[1,2], FANG Ronghui[3,4], BORJIGIN Tenger[3,4], XIAO Hong[1,2], ZHU Zhili[5]

1. State Key Laboratory of Petroleum Resources and Prospecting, China University of Petroleum (Beijing), Beijing 102249, China;
2. College of Geosciences, China University of Petroleum (Beijing), Beijing 102249, China;
3. Oil and Gas Survey, China Geological Survey, Beijing 100083, China;
4. Key Laboratory of Unconventional Oil & Gas Geology Center, China Geological Survey, Beijing 100083, China;
5. Wuxi Research Institute of Petroleum Geology, SINOPEC, Wuxi 214126, Jiangsu

Abstract: Laser Raman spectroscopy has shown a good application prospect for maceral analysis. Raman spectroscopic analysis of different macerals (e. g., vitrinite, semifusinite and macrinite) in coal samples with different maturity (%R_o = 0.49%–1.88%) was carried out in this study, and results show that three macerals have significantly different Raman spectrum parameters, which have the following implications for the macerals analysis of coal: (1)Macerals in coal samples can be distinguished by the combination of Raman spectrum parameters. There are 21 kinds of parameter combinations discussed in this study, which can be used as reference standard for the classification of these organic macerals; (2) Peak displacement (W_{D1}) is the most critical parameter to distinguish the macerals of coal samples. The influence of thermal evolution should be considered, which may assistant for the study of maceral differences in the Lower Paleozoic which are in the high to over mature stage with optical properties gradually converging. Therefore, Raman spectrum parameters can be used as an effective method for maceral analysis.
DOI: 10.11781/sysydz202204705-en

Keywords: macerals; maturity; Raman spectrum parameters; coal sample

Macerals classification is of great significance to the identification of organic matter types in source rocks and the study of pores [1–3] in shale gas reservoirs. Although the research method has developed from optical microscope to scanning electron microscope with higher resolution [1, 4–5], the analysis of organic macerals has always been dominated by traditional manual identification, which makes the results greatly affected by human factors such as the polishing quality of light sheets and the ability of researchers. In recent years, the Lower Paleozoic marine shale has become a research hotspot [6]. Among the marine shale, most of its organic matter is in the high to over mature stage [7–9] with optical properties gradually converged, making it difficult to be identified by using traditional manual analysis methods [10].

Raman spectroscopy, as a microstructure analysis method, can reflect the ordering and structural defects of the structure during the thermal evolution of graphitized carbon materials, thus achieving a wide use in oil and gas geological research in recent years [10–25]. The chemical structure of different macerals in coal differs from each other [26]. As the coalification deepens, its carbonaceous structure gradually becomes ordered [27]. Therefore, Raman spectroscopy can be used to study coal macerals from the microstructure to effectively reduce the analysis error caused by human factors and provide reference for the study of shale maceral differences.

In this paper, coal samples with different thermal maturity were selected to study the variation characteristics of Raman spectrum parameters of coal macerals, and the Raman spectrum parameters of several main macerals in the selected coal samples were preliminarily studied in order to explore the method of using Raman spectrum parameters to effectively analyze different coal macerals.

1 Experimental samples and methods

1.1 Sample collection and preparation

In this paper, 10 humic coal samples (measured vitrinite reflectance R_o = 0.55%–1.88%) from the Carboniferous-Permian outcrop in the eastern Ordos Basin and 2 humic coal

Received: 2021-07-07
Supported by: National Geological Survey and Evaluation Special Project "Oil and gas geological survey drilling core preservation parameter acquisition and application" (DD20201114)
First author: GAO Zhiwei (1996–), male, master, engaged in oil and gas geochemistry research. E-mail: 2019215032@student.cup.edu.cn.
Corresponding author: LI Meijun (1972–), male, doctor, professor, engaged in oil and gas geochemistry research. E-mail: meijunli@cup.edu.cn.

samples (measured vitrinite reflectance R_o = 0.82%–1.08%) from the Jurassic outcrop in the southeastern Junggar Basin with organic matters of types II and III were selected.

Sample preparation: the samples were prepared into 2 cm × 2 cm blocks with one flat side, then put the samples in a fixed sharpener and poured epoxy resin into it for condensation and curing. After complete curing, it was ground and polished with Buehler EcoMet/AutoMet 300 automatic grinder-polisher and aluminum oxide polishing solution. The experiment was carried out after the samples were completely dry.

1.2 Experimental instruments and conditions

Experimental instruments: the experiment was conducted by the Renishaw inVia laser micro confocal Raman spectrometer with spectral resolution of 2 wave numbers and instrument resolution of 1 μm. The excitation light source was an argon ion laser (the laser wavelength is 532 nm), the grating is 1 800 lines, and the slit is 65.1 μm. Raman spectrum parameters were calculated by the built-in spectrum analysis software WIRE4.1. The experiment was performed under lights-off conditions.

Experimental conditions: Silicon chip was used for wave number calibration. The test started when the Raman displacement of monocrysta line silicon was (520 ± 0.5) cm^{-1} after half an hour's available machine time. Researches have showed that high power laser Raman experiments will cause changes in Raman spectrum parameters and even damage the surface structure of organic matters [14]. Before the experiment, the experimental power was tested on the sample macerals, and the maximum power that macrinite, semifusinite, and vitrinite could bear was tested to be 1%, 5%, and 0.05% respectively. In this experiment, the final test power was set to be 0.05% (the exciter power is 10 mW); the single point continuous scanning was used with scanned area of 100–3 500 cm^{-1}; the exposure time was 10 s, which was accumulated for 5 times; and linear baseline was adopted in the curve fitting process.

2 Spectrum processing parameters setting

2.1 Pretreatment parameters setting

The influence of noise is inevitable in Raman spectrum experiments [28], so pretreatment methods are needed to remove the noise before the final selection of Raman spectrum parameters. Software WIRE4.1 was used in this paper to preprocess the spectrum, and the pretreatment methods include smoothing processing and baseline correction. See Table 1 for the optimization of pretreatment parameters and results of laser Raman spectroscopy.

2.2 Curve fitting parameters setting

Currently, there is no unified standard for curve fitting. In order to obtain a better fitting, previous studies have developed from two peak fitting to multi peak fitting [11, 16, 29–30]. In this paper, the first-order peak is divided into five peaks (Fig. 1), including D1, D2, D3, D4, and G, and then the Raman spectrum parameters are calculated. Since the position of D1 peak and G peak is less affected by peak fitting, the parameters related to D1 peak and G peak are selected when using parameters. In this paper, the fitting peak parameters are not limited in the specific fitting, which can best fit the Raman spectrum [31].

3 Results and discussion

3.1 Raman spectral characteristics of different macerals in the sample

The organic macerals in sample 2 (R_o = 0.62%) mainly include semifusinite, macrinite and vitrinite (Fig. 2), which are detected by Raman spectroscopy respectively. It can be seen from the Raman spectra (Fig. 3) that the first-order regions (1 000–1 800 cm^{-1}) of the Raman spectra of different macerals all contain two main peaks: the disordered peak (D) (about 1 340 – 1 360 cm^{-1}) and the graphite peak (G) (about 1 580 cm^{-1}), in which the D peak is related to the lattice defects and disorder of organic matter, and the G peak is related to the vibration between C–C on the aromatic configuration plane in the graphite structure [21]. There is a significant difference among the baseline slopes of semifusinite, macrinite, and vitrinite (Fig. 3a). Vitrinite has a larger baseline slope and is more strongly affected by fluorescence [12]. There are slight differences between the baseline slopes of semifusinite and macrinite, but the differences are not obvious.

Raman spectrum parameters of different macerals in sample 2 are different before and after Raman spectrum pretreatment (Fig. 3, Table 2). Table 2 shows that from vitrinite to semifusinite and macrinite, the peak displacement W_{D1} and half peak breadth FWHM-D1 decrease in turn, indicating that the structural defects and the degree of disorder decrease in turn. The peak displacement is almost unchanged, and the half peak breadth FWHM-G has no consistent law but shows a characteristic of inertinite smaller than vitrinite on the whole, indicating that the graphitization degree of inertinite is stronger than that of vitrinite. The peak displacement difference (*RBS*) is positively correlated with the degree of condensation of aromatic rings in the molecular structure of organic matters [13]. *RBS* of different macerals shows the law of vitrinite < semifusinite < macrinite, indicating that the degree of condensation of aromatic rings gradually increases from vitrinite to semifusinite and macrinite.

3.2 Characteristics of Raman spectrum parameters of macerals with different maturity

Laser Raman detection was performed on the main macerals in samples with different thermal maturity (R_o =

0.55%–1.88%), and the relevant Raman spectrum parameters were counted (Table 3). It can be found from Table 3 that there is almost no change in peak displacement W_G among different macerals, while W_{D1} shows an obvious characteristic of vitrinite > semifusinite > macrinite, in which the variation ranges of vitrinite, semifusinite, and macrinite are 1 359–1 378 cm^{-1}, 1 355–1 358 cm^{-1}, and 1 341–1 352 cm^{-1} respectively, indicating that the structural defects and disorder degree decrease from vitrinite to semifusinite and macrinite in turn. The variation law of peak displacement difference of different macerals is opposite, appearing as vitrinite < semifusinite < macrinite, indicating that the degree of condensation of aromatic rings gradually increases from vitrinite to semifusinite and macrinite. Half peak breadth FWHM-D1 of different macerals has no obvious change, and the variation ranges of FWHM-G of macrinite and semifusinite are 57–65 and 57–69 respectively with slight difference, but generally smaller than that of vitrinite (62–81), indicating that the graphitization degree of inertinite is stronger than that of vitrinite. Moreover, as thermal evolution increases, the difference in Raman spectrum parameters of different coal macerals gradually decreases and tends to be consistent, indicating that the homogeneity of coal samples is becoming stronger and stronger.

Table 1 Optimization of pretreatment parameters and results of laser Raman spectroscopy

Parameter optimization and results		Smoothing processing		Baseline correction	
		Smoothing window	Polynomial fitting order	Smoothing times	Polynomial fitting order
Fixed parameters		Smoothing window=9	Polynomial fitting order=3	Smoothing window=9, fitting order=6	Smoothing with optimized parameters
Variable parameters		Smoothing window=5–99	Fitting order=2–8	Smoothing times=1–10	Fitting order=1–12
Fitting effect comparison	Spectroscopy	Visual comparison between processed spectroscopy and original spectroscopy			
	Spectroscopic parameters/bimodal fitting	I_D/FWHM-D, I_G/FWHM-G, *RBS*, R_1, saddle index (SI)			
Parameter optimization results		Smoothing window=9	Fitting order=6	Smoothing times=1	Fitting order=3

Note: I_{D1} and I_G are the peak intensities of D1 peak and G peak respectively; FWHM-D1 and FWHM-G are the half peak breadths of D1 peak and G peak respectively; Peak displacement difference $RBS = W_G - W_{D1}$ (W_{D1} and W_G are the peak displacements of D1 peak and G peak respectively); Peak intensity ratio $R_1 = I_{D1}/I_G$; *SI* is the saddle index.

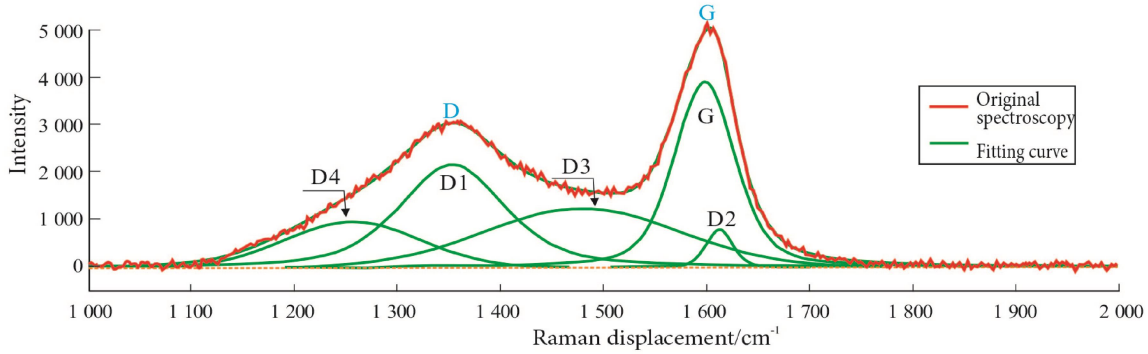

Fig. 1 Fitting results of Raman spectra of macrinite in sample 2

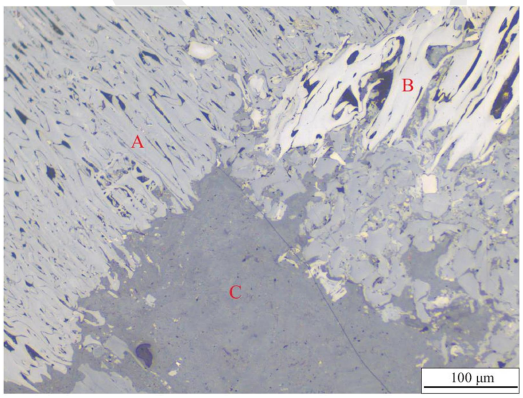

Fig. 2 Micrographs of various organic macerals in sample 2

A. Semifusinite; B. Macrinite; C. Vitrinite

3.3 Application of Raman spectrum parameters in distinguishing organic macerals

From the above analysis, it can be seen that the Raman spectrum parameters of different macerals are different, so Raman spectrum parameters can be used to distinguish macerals. By introducing the thermal maturity factor, statistics were made on the correlation between Raman spectrum parameters and vitrinite reflectance R_o, the results of distinguishing macerals (semifusinite, macrinite, and vitrinite) by combining Raman spectrum parameters with R_o, and the results of combining Raman spectrum parameters related to R_o in pairs (Table 4, some graphs are shown in Fig. 4), and it was found that there are 21 kinds of parameter combinations that can distinguish the macerals in the sample: 3 of them are

combinations of Raman spectrum parameters and R_o (W_{D1}–R_o, W_{D1}/W_G–R_o, RBS–R_o); and the other 18 are combinations of different Raman spectrum parameters (W_{D1}–W_G, W_{D1}–FWHM-D1, W_{D1}–FWHM-G, W_{D1}–R_1, W_{D1}–A_{D1}/A_G, W_{D1}/W_G–W_G, W_{D1}/W_G–FWHM-D1, W_{D1}/W_G–FWHM-G, W_{D1}/W_G–R_1, W_{D1}/W_G–A_{D1}/A_G, RBS–W_G, RBS-FWHM–D1, RBS–FWHM-G, RBS–R_1, RBS–A_{D1}/A_G, W_{D1}–RBS, W_{D1}–W_{D1}/W_G, RBS–W_{D1}/W_G).

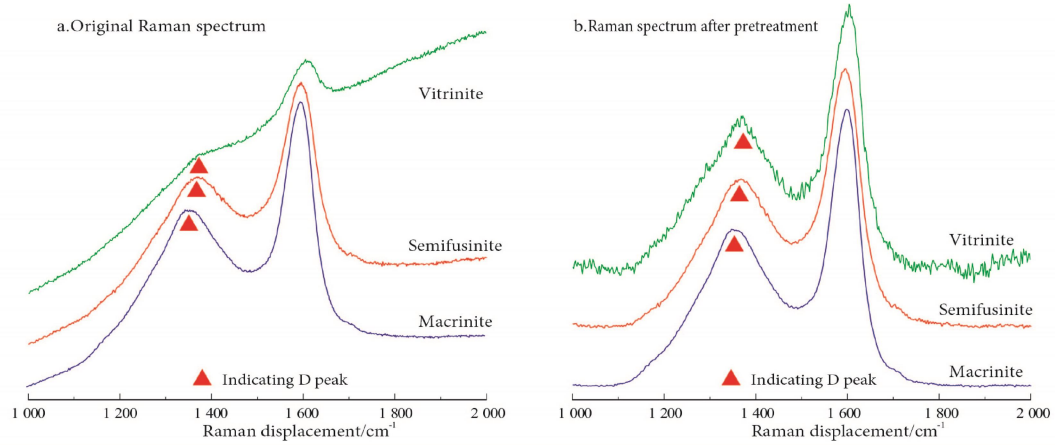

Fig. 3 Raman spectra of different organic macerals in sample 2

Table 2 Raman spectroscopic parameters of different macerals in sample 2

Macerals	D1 peak		G peak		RBS/cm^{-1}
	W_{D1}/cm^{-1}	FWHM-D1	W_G/cm^{-1}	FWHM-G	
Vitrinite	1 364.32	112.89	1 597.07	68.32	232.75
Semifusinite	1 357.74	108.27	1 598.93	63.54	241.20
Macrinite	1 350.03	101.95	1 597.02	67.04	246.99

Table 3 Raman spectroscopic parameters of macerals in different maturity samples

Sample No.	R_o/%	Macerals	W_{D1}/cm^{-1}	FWHM-D1	W_G/cm^{-1}	FWHM-G	RBS/cm^{-1}
1	0.55	Macrinite	1 349.95	121.35	1 598.37	69.28	248.42
		Semifusinite	1 358.20	119.56	1 598.66	65.77	240.46
		Vitrinite	1 378.85	125.58	1 599.34	81.47	220.49
2	0.62	Macrinite	1 350.03	101.95	1 597.02	67.04	246.99
		Semifusinite	1 357.74	108.27	1 598.93	63.54	241.20
		Vitrinite	1 364.32	112.89	1 597.07	68.32	232.75
3	0.71	Semifusinite	1 358.08	117.01	1 595.66	63.89	237.58
4	0.82	Macrinite	1 351.68	127.99	1 598.52	63.75	246.84
		Vitrinite	1 373.53	134.41	1 587.56	73.08	214.03
5	0.96	Vitrinite	1 368.28	104.56	1 597.78	68.66	229.50
6	1.08	Macrinite	1 352.35	110.36	1 598.30	63.85	245.95
		Semifusinite	1 357.83	101.52	1 598.74	65.93	240.91
		Vitrinite	1 367.97	109.03	1 597.90	67.72	229.92
7	1.24	Macrinite	1 348.16	109.21	1 599.75	61.89	251.59
		Vitrinite	1 365.59	100.59	1 597.66	63.81	232.07
8	1.35	Macrinite	1 343.26	121.59	1 599.48	63.50	256.22
		Vitrinite	1 365.16	94.76	1 598.16	63.68	233.01
9	1.40	Macrinite	1 347.80	111.51	1 598.63	62.29	250.84
		Semifusinite	1 354.76	65.68	1 594.82	64.93	240.06
		Vitrinite	1 359.56	94.57	1 595.57	62.26	236.01
10	1.57	Macrinite	1 342.28	119.04	1 599.25	59.26	256.97
		Semifusinite	1 352.23	89.18	1 599.60	57.44	247.36
11	1.66	Macrinite	1 341.46	117.85	1 600.30	58.52	258.84
		Semifusinite	1 357.41	86.01	1 600.08	60.35	242.67
12	1.88	Macrinite	1 351.09	90.00	1 598.33	57.40	247.24
		Semifusinite	1 355.38	92.07	1 600.55	57.61	245.17

Table 4 Combination of Raman spectral parameters for the classification of macerals (R_o = 0.55%–1.88%)

Combination type	Parameter	Correlation with R_o	Whether the combination can distinguish macerals	Combination type	Correlation with W_{D1}	Combination parameters		Whether the combination can distinguish macerals
Basic parameter -R_o	W_{D1}	-	Y	Parameters - parameters	0	W_G, FWHM-D1, FWHM-G, R_1, A_{D1}/A_G	W_G, FWHM-D1, FWHM-G, R_1, A_{D1}/A_G	N
	W_G	+	N					
	I_{D1}	- -	N					
	I_G	- -	N					
	A_{D1}	- -	N		1	W_{D1}, W_{D1}/W_G, *RBS*	W_G, FWHM-D1, FWHM-G, R_1, A_{D1}/A_G	Y
	A_G	- -	N					
	FWHM-D1	-	N					
	FWHM-G	-	N					
Derived parameter -R_o	W_{D1}/W_G	-	Y		2	W_{D1}, W_{D1}/W_G, *RBS*	W_{D1}, W_{D1}/W_G, *RBS*	Y
	RBS	+	Y					
	R_1	+	N					
	A_{D1}/A_G	+	N					

Note: ① A_{D1} and A_G are the peak areas of D1 peak and G peak respectively, and the peak intensity ratio R_1= I_{D1}/I_G; ② Correlation with W_{D1} refers to the number of parameters containing W_{D1} or derived parameters of W_{D1} (W_{D1}/W_G, *RBS*); ③- refers to negative correlation, + refers to positive correlation, -- refers to poor correlation; ④ Combination parameter refers to the Raman spectrum parameter related to the thermal maturity R_o.

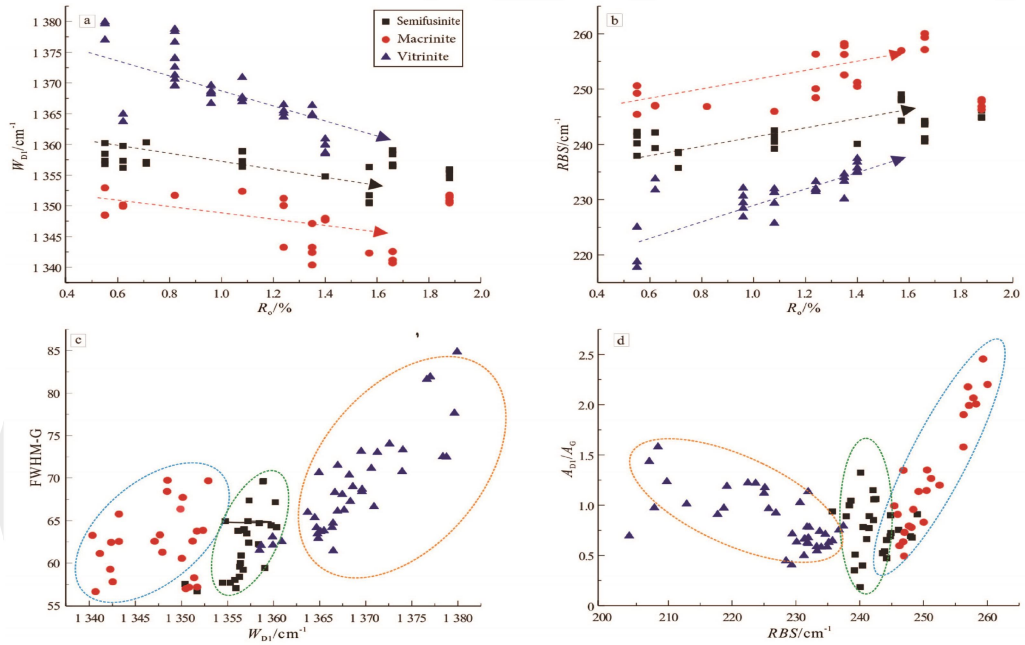

Fig. 4 Combination of Raman spectral parameters for the classification of macerals

Through analysis, it can be seen that among all of the Raman spectral parameter combinations that can distinguish macerals, at least one parameter should be W_{D1} or derived parameters of W_{D1} (W_{D1}/W_G, *RBS*), while W_{D1} and its derived parameters are mainly controlled by thermal maturity. Therefore, the influence of thermal maturity needs to be considered when distinguishing macerals by Raman spectrum parameters.

Based on this conclusion, the author counted the relevant parameters of samples with different macerals in Lower Paleozoic marine source rocks in some literatures and drew the relevant graphs (Fig. 5). From the literature, we can see that the evolution of $W_{D1/D}$ of vitrinite, asphalt and graptolite with thermal maturity R_o is similar. in case that the Lower Paleozoic marine source rocks lack vitrinite from higher plants, being new thermal maturity indicators, asphalt and graptolite have become a research hotspot. In addition, the $W_{D1/D}$ of graptolite, solid asphalt, benthic algae, and planktonic algae are different in the process of thermal evolution, which may assistant for the identification of organic macerals in the Lower Paleozoic that are in the high to over mature stage with optical properties gradually converging.

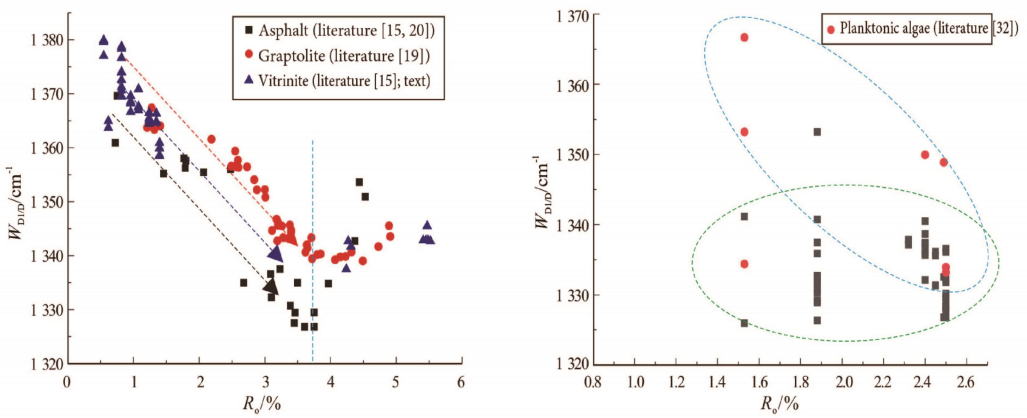

Fig. 5 Parameter characteristics of different macerals in literature

4 Conclusions

Through the study on laser Raman parameters of three main macerals (vitrinite, semifusinite, and macrinite) in a total of 12 coal samples (R_o = 0.55%–1.88%) from the Carboniferous-Permian in the eastern Ordos Basin and the Jurassic in the southeastern Junggar Basin, the following understandings are obtained:

(1) The three macerals in the selected coal samples have significantly different Raman spectrum parameters. There are 21 kinds of parameter combinations that can distinguish the macerals in the sample: 3 of them are combinations of Raman spectrum parameters and R_o, and the other 18 are combinations of different Raman spectrum parameters. All these different combinations of parameters can be used as reference standards for the classification of these organic macerals.

(2) D1 peak displacement (W_{D1}) is the most critical parameter to distinguish the macerals by Raman spectrum parameters, but the influence of thermal evolution should be considered, which may help the identification of Lower Paleozoic organic macerals in the high to over mature stage with optical properties gradually converging.

Acknowledgements

Acknowledgment: We hereby express our sincere thanks to Dr. QIN from the National Research Center for Geoanalys for her corresponding experimental help in the identification of coal macerals!

References

[1] ZHANG Hui, JIAO Shujing, PANG Qifa, et al. SEM observation of organic matters in the Eopaleozoic shale in South China [J]. Oil & Gas Geology, 2015, 36 (4): 675–680.

[2] GAO Fenglin, SONG Yan, LIANG Zhikai, et al. Development characteristics of organic pore in the continental shale and its genetic mechanism: a case study of Shahezi Formation shale in the Changling Fault Depression of Songliao Basin [J]. Acta Petrolei Sinica, 2019, 40 (9): 1030–1044.

[3] YANG Yunfeng, BAO Fang, BORJIGIN T, et al. Characteristics of organic matter hosted pores in Lower Silurian Longmaxi shale with different maturities, Sichuan Basin [J]. Petroleum Geology & Experiment, 2020, 42 (3): 387–397.

[4] JIAO Shujing, ZHANG Hui, XUE Dongchuan, et al. Morphological structure and identify method of organic macerals of shale with SEM [J]. Journal of Chinese Electron Microscopy Society, 2018, 37 (2): 137–144.

[5] GAO Fenglin, WANG Chengxi, SONG Yan, et al. Ar-ion polish-ing FE-SEM analysis of organic maceral identification [J]. Petroleum Geology & Experiment, 2021, 43 (2): 360–367.

[6] ZHAI Gangyi, WANG Yufang, BAO Shujing, et al. Major factors controlling the accumulation and high productivity of marine shale gas and prospect forecast in Southern China [J]. Earth Science, 2017, 42 (7): 1057–1068.

[7] XU Xuemin, SUN Weilin, WANG Shuangqing, et al. Maturity evaluation of marine shale in the Lower Paleozoic in South China [J]. Earth Science, 2019, 44 (11): 3717–3724.

[8] CHEN Shangbin, ZUO Zhaoxi, ZHU Yanming, et al. Applicability of the testing method for the maturity of organic matter in shale gas reservoirs [J]. Natural Gas Geoscience, 2015, 26 (3): 564–574.

[9] CHENG Peng, XIAO Xianming. Gas content of organic-rich shales with very high maturities [J]. Journal of China Coal Society, 2013, 38 (5): 737–741.

[10] LUO Qingyong, HAO Jingyue, LI Kewen, et al. A new parameter for the thermal maturity assessment of organic matter from the Lower Palaeozoic sediments: a re-study on the optical characteristics of graptolite periderms [J]. Acta Geologica Sinica, 2019, 93 (9): 2362–2371.

[11] HENRY D G, JARVIS I, GILLMORE G, et al. Raman spectroscopy as a tool to determine the thermal maturity of organic matter: application to sedimentary, metamorphic and structural geology [J]. Earth-Science Reviews, 2019, 198: 102936.

[12] BAO Fang, TENGGER, YANG Yunfeng, et al. Raman spectroscopic characteristics of different hydrocarbon-forming organisms [J]. Geological Journal of China Universities, 2012, 18 (1): 174–179.

[13] BAO Fang, LI Zhiming, ZHANG Meizhen, et al. Application of laser Raman spectrum in organic maceral studies [J]. Petroleum Geology & Experiment, 2012, 34 (1): 104–108.

[14] HENRY D G, JARVIS I, GILLMORE G, et al. Assessing low-maturity organic matter in shales using Raman spectroscopy: effects of sample preparation and operating procedure [J]. International Journal of Coal Geology, 2018, 191: 135–151.

[15] LIU Dehan, XIAO Xianming, TIAN Hui, et al. Sample maturation calculated using Raman spectroscopic parameters for solid organics: methodology and geological applications [J]. Chinese Science Bulletin, 2013, 58 (11): 1 285–1 298.

[16] XIAO Xianming, ZHOU Qin, CHENG Peng, et al. Thermal maturation as revealed by micro-Raman spectroscopy of mineral-organic aggregation (MOA) in marine shales with high and over maturities [J]. Science China Earth Sciences, 2020, 63 (10): 1 540–1 552.

[17] WILKINS R W T, BOUDOU R, SHERWOOD N, et al. Thermal maturity evaluation from inertinites by Raman spectroscopy: the 'RaMM' technique [J]. International Journal of Coal Geology, 2014, 128–129: 143–152.

[18] WILKINS R W T, WANG M, GAN H J, et al. A RaMM study of thermal maturity of dispersed organic matter in marine source rocks [J]. International Journal of Coal Geology, 2015, 150–151: 252–264.

[19] WANG Ye, QIU Nansheng, BORJIGIN T, et al. Integrated assessment

of thermal maturity of the Upper Ordovician-Lower Silurian Wufeng–Longmaxi shale in Sichuan Basin, China [J]. Marine and Petroleum Geology, 2019, 100: 447–465.
[20] WANG Maolin, XIAO Xianming, WEI Qiang, et al. Thermal maturation of solid bitumen in shale as revealed by Raman spectroscopy [J]. Natural Gas Geoscience, 2015, 26 (9): 1 712–1 718.
[21] ZUO Zhaoxi, CHEN Shangbin, SHI Qian, et al. Application of laser Raman spectroscopy to the evaluation of the high- and overhigh-maturity of shale and coal [J]. Rock and Mineral Analysis, 2016, 35 (2): 193–198.
[22] XU Chang, YAO Suping, SONG Di, et al. Types, chemical and porosity characteristics of hydrocarbon-generating organisms of the Lower Paleozoic, South China: taking Longmaxi Formation and Qiongzhusi Formation in Sichuan Basin as examples [J]. Marine and Petroleum Geology, 2020, 119: 104 508.
[23] ZHANG Cong, XIA Xianghua, YANG Yuru, et al. Raman spectrum characteristics of organic matter in Silurian Longmaxi Formation shale of well Anye-1 and its geological significance [J]. Rock and Mineral Analysis, 2019, 38 (1): 26–34.
[24] TIAN Ye, TIAN Yuntao. Fundamentals and applications of Raman Spectroscopy of Carbonaceous Material (RSCM) thermometry [J]. Advances in Earth Science, 2020, 35 (3): 259–274.
[25] HAO Jingyue, ZHONG Ningning, LUO Qingyong, et al. Raman spectroscopy of graptolite periderm and its potential as an organic maturity indicator for the Lower Paleozoic in southwestern China [J]. International Journal of Coal Geology, 2019, 213: 103278.
[26] WANG Qiang, MAO Ning, YANG Yan, et al. Molecular structures and comparative analysis of macerals of vitrinite and inertinite for Qinghua coal, Ningxia [J]. Chemical Industry and Engineering Progress, 2020, 39 (S2): 142–151.
[27] CAO Daiyong, WEI Yingchun, WANG Anmin, et al. The evolution difference of macromolecular structures and its dynamic mechanism of coal macerals: research status and prospect [J]. Coal Geology & Exploration, 2021, 49 (1): 12–20.
[28] BOCKLITZ T, WALTER A, HARTMANN K, et al. How to pre-process Raman spectra for reliable and stable models? [J]. Analytica Chimica Acta, 2011, 704 (1/2): 47–56.
[29] SCHITO A, ROMANO C, CORRADO S, et al. Diagenetic thermal evolution of organic matter by Raman spectroscopy [J]. Organic Geochemistry, 2017, 106: 57–67.
[30] FERRALIS N, MATYS E D, KNOLL A H, et al. Rapid, direct and non-destructive assessment of fossil organic matter via micro Raman spectroscopy [J]. Carbon, 2016, 108: 440–449.
[31] SAUERER B, CRADDOCK P R, ALJOHANI M D, et al. Fast and accurate shale maturity determination by Raman spectroscopy measurement with minimal sample preparation [J]. International Journal of Coal Geology, 2017, 173: 150–157.
[32] LI Miaochun. The organic petrology and geological significance of Lower Paleozoic source rock: a case study of what in Upper Yangtze region [D]. Nanjing: Nanjing University, 2014.

